

# A Closed-Form Solution for Kernel Adaptive Filtering

Benjamin Lyons Colburn<sup>a</sup>, Luis G. Sanchez Giraldo<sup>b</sup>, Kan Li<sup>a</sup>,  
and Jose C. Principe<sup>a</sup>

<sup>a</sup>Department of Electrical and Computer Engineering, University of Florida

<sup>b</sup> Department of Electrical and Computer Engineering, University of Kentucky

## Abstract

Conventional kernel adaptive filtering (KAF) uses a prescribed, positive-definite, nonlinear function to define the Reproducing Kernel Hilbert Space (RKHS), where the minimum mean square error solution is found using search techniques. This paper proposes embedding the statistics of the input data in the kernel definition, obtaining a closed-form solution for nonlinear adaptive filtering applications. We call this solution the Functional Wiener Filter (FWF), which extends Parzen's work on the autocorrelation RKHS to nonlinear functional spaces. We first derive a space-time covariance operator on a RKHS that generalizes Parzen's autocovariance RKHS and includes nonlinear functions of a random process. We then present a method for approximating the FWF in an explicit, finite-dimensional RKHS to model time series directly from realizations. The FWF can be computed in closed form directly from realizations and has better accuracy than other kernel-based algorithms in a synthetic strictly stationary dataset. We show that FWF performance is comparable to other KAF algorithms for two chaotic time series and a real-world time series. The FWF's computational complexity at test time is an improvement over other KAFs. We demonstrate how the difference equation learned by the FWF can be extracted, leading to system identification applications, beyond optimal nonlinear filtering.

# 1 Introduction

In 1949, Norbert Wiener published his book, "Extrapolation, Interpolation, and Smoothing of Stationary Time Series" [38], where he detailed his seminal work on linear minimum mean squared error (MMSE) estimation. While this work launched statistical modeling of time series, the Wiener-Hopf method [39] is rather complex and the optimal solution still belongs to the span of the input data i.e., the corresponding model is linear.

Briefly, let  $X$  be a wide-sense multivariate stationary random process, and  $Z$  be a target measurement of a multivariate random variable. Define the error  $e = Z - \hat{Z}$ , where  $\hat{Z}$  is any arbitrary function of  $X$  and  $Z$ , called the estimator. By definition, the mean square error (MSE) is the trace of the autocorrelation of the error  $\mathbb{E}[ee^\top]$ . The MMSE estimator finds the  $\hat{Z}$  which minimizes this trace. Alternatively, the minimal MSE can be found using gradient descent techniques, with the advantage of allowing nonlinear mapping functions of  $X$ , but the solution is neither closed-form nor unique. In a Bayesian setting, the MMSE estimator is given by the posterior mean. Since the posterior mean involves an integration, the form of the MMSE estimator is usually constrained to be within a certain class of functions if a closed-form solution is desired. Linear MMSE estimators are in widespread use in statistics and signal processing in part because they allow for a closed-form solution and provide a simple interpretation of the learned model. The main contribution of this paper is the construction of a reproducing kernel Hilbert space (RKHS) to solve the posterior mean analytically as a minimum norm projection, yielding a closed-form solution for nonlinear MMSE estimation that differs from the ones available in the literature.

In the late 50s, Emmanuel Parzen [25] presented an alternative approach to solve the linear MMSE problem in a RKHS defined by the autocovariance function of a wide-sense stationary random process (r.p.). He shows that the MMSE solution in this RKHS is exactly the inner product of the input time series with the cross-covariance function between the input time series and the desired time series.

Parzen argues that the embedding of the statistical information of the autocovariance function into the inner product of the RKHS creates a natural space for statistical inference on time series because conditional expectations with respect to the stationary input r.p. can be expressed as inner products in the space (under some Gaussian assumptions). This claim of a "natural" space is supported by the subsequent use of the autocovariance RKHS( $\mathcal{H}_R$ )

to clarify and simplify many problems such as the detection of deterministic signals in colored Gaussian noise [13], detection of Gaussian signals in Gaussian noise [12], generalized innovations representations [11], calculation of the likelihood-ratio in Gaussian [11] and non-Gaussian settings [4], and parameter estimation [5].

This paper takes Parzen’s theoretical work one step further by deriving a closed-form solution for a nonlinear MMSE estimator in a data-dependent RKHS. Inspired by [25], we also project the input data to a RKHS, but now the kernel is data-dependent and nonlinearly related to the input space. While Kernel Adaptive Filtering (KAF) [17] poses the problem of nonlinear MMSE filter design as a search in an RKHS defined by a data-independent, nonlinear kernel, the proposed method is quite different. It first designs a data-dependent universal RKHS and then computes, in closed-form, the minimum norm projection of the target in the constructed space, avoiding gradient search. While a closed-form solution to select parameters of a nonlinear filter for regression is foundational in its own right, the method for embedding the statistics of input data, i.e. its internal dependency structure, into the inner product of an RKHS defined by a nonlinear kernel is perhaps the more generally applicable contribution of this work.

To achieve our goal, we show that full access to individual eigenfunctions of the kernel is necessary, which is beyond the reach of the conventional “kernel trick” [31]. Instead, for the implementations, we approximate the Gaussian kernel by an explicit, finite-dimensional RKHS where the inner product becomes an explicit quadratic form of vectors. The disadvantage is that the explicit RKHS is finite-dimensional i.e., no longer universal or characteristic. However, the previous results in [14] show that only a few dimensions are needed to achieve excellent performance with KAF algorithms.

The main contributions of this work are the following:

- We introduce an extension of Parzen’s MMSE in  $\mathcal{H}_R$  to an RKHS that includes nonlinear functions of a time series, yielding a closed-form, computationally efficient, and effective nonlinear MMSE estimator.
- We provide a method for the practical implementation and use of a data-dependent nonlinear RKHS for signal processing applications.
- We show experimentally that if the assumptions made in the closed-form solution are met we outperform other kernel-based nonlinear filtering methods.

- We show that the optimal solution parameters can be interpreted as a nonlinear difference equation learned directly from the data. This extends possible applications of the method to system identification tasks and physics based modeling in RKHS.

We will highlight some more related works next. In [37] a comprehensive treatment of spline models is given. The problem of finding an optimal MMSE spline to fit data is presented in an RKHS, however, the formulation of the solution is quite different from ours in that our solution first focuses on defining a nonlinear data-dependent space where the MMSE solution can be immediately given. In [4] the idea of a covariance function is extended to a characteristic functional, which under certain conditions can characterize non-Gaussian r.p.s. (see [9] for a description of the characteristic functional). This is related to our work in that it seeks to define a data-dependent RKHS. While the results in [4] are theoretically interesting, the conditions are restrictive, and its application to general problems such as MMSE filtering is not clear.

More contemporary related work is centered on Kernel Adaptive Filtering (KAF). A comprehensive description of the foundational work can be found in [17]. In general, KAF utilizes gradient search methods to find the optimal functional in the feature space of an RKHS resulting in a nonlinear filter. Some examples of this approach are Kernel Least Mean Squares (KLMS) [16] and Kernel Recursive Least Squares [6] which extend the least mean squares and recursive least squares algorithms respectively.

The strength of many KAF methods is that they are convex universal learning machines with simple implementations. One of the main issues with KAF is that the model size grows with the number of training samples. This problem is addressed by sparsification algorithms such as Quantized Kernel Least Mean Squared (QKLMS) [1]. A comparative study of different KAF techniques with sparsification can be found in [36]. Another notable strategy for decoupling model size with the number of training samples is to use finite-dimensional approximations of the feature space specified by some reproducing kernel. Examples of this can be found in [14], [28], and [18]. In our work, we utilize this finite-dimensional approximation, which decouples model size from training set size. Our method is distinct from other KAF methods in a few consequential ways. Firstly, we eliminate the need for an iterative gradient-based search through an RKHS, hence our claim of a closed-form solution for KAF. Second, while other KAF methods define a

functional based solely on the amplitude of a time series, the FWF yields functionals over both time and amplitude values. Third, the FWF focus on first building a data-dependent RKHS where the MMSE solution can immediately be given. This is a fundamentally different approach to solving for a MMSE solution.

Another popular kernel-based regression method is Gaussian Process Regression (GPR) [29]. This method uses a Gaussian Process (a time series where all joint distributions are Gaussian) to define a distribution over possible functions. Then the data is used to update this prior distribution using maximum a posteriori (MAP) estimators. GPR offers a Bayesian framework for nonlinear regression, which is distinct from the adaptive filtering-based framework of KAF.

In [23], the kernel autocovariance operators of stationary processes are theoretically studied, and classical limit theorems as well as non-asymptotic error bounds under some ergodic assumptions are discussed. The authors also give a conditional mean operator based on the autocovariance operator. The autocovariance operators discussed in [23] are closely related to the  $U$  operator discussed in later sections of this text. However, [23] is focused on the analysis of the kernel autocovariance operator itself, while our work was independently developed and progresses in the opposite direction. It starts with the foundational ideas of statistical signal processing developed by Wiener, Parzen, and KAF and extends all these concepts to potentially universal data-dependent RKHS and covariance operators. We believe that our approach will be easier to understand by experts in signal processing. Moreover, it provides algorithms for practical applications that can be easily understood and employed by practitioners.

## 2 MMSE Solutions in Data-Dependent RKHSs

### 2.1 Random Processes

Let  $(\Omega, \mathcal{A}, P)$  be a probability space with sample space  $\Omega$ ,  $\sigma$ -algebra  $\mathcal{A}$ , and probability measure  $P$ . A random process (r.p.),  $X = \{X_t, t \in T\}$ , is a collection of random variables (r.v.s.) defined on,  $(\Omega, \mathcal{A}, P)$ , along with an index set  $T$  that is a compact subset of a separable metric space usually representing time. All r.p.s. will be assumed to contain real-valued r.v.s.. We denote a single r.v. within a r.p. with a capital letter subscripted with

its index,  $X_t$ . Realizations from these random variables will be denoted as  $x_t$ .

In our treatment of the linear MMSE solution, we assume wide-sense stationarity of the processes involved. A wide-sense stationary random process satisfies the following relation [33],

$$R(\tau) = \mathbb{E}[X_t X_{t-\tau}] \quad (1)$$

for any  $t \in T$  and  $\tau$  such that  $t - \tau \in T$ . Likewise, for two jointly stationary random processes  $Z$  and  $X$ ,

$$\rho(\tau) = \mathbb{E}[Z_t X_{t-\tau}] \quad (2)$$

for any  $t \in T$  and  $\tau$  such that  $t - \tau \in T$ . In other words, the joint second-order statistics are independent of  $t$ . This assumption of wide-sense stationarity is necessary to practically estimate the necessary quantities needed to solve the Wiener-Hopf equations from realizations of a random process [38]. Another important notion of stationarity is strict stationarity. A strictly stationary random process is a r.p. where the joint distributions(not just the second-order moments) do not change with shifts in time. This strict stationarity assumption will become important in the nonlinear MMSE solution.

## 2.2 Linear MMSE Solution

We now review the linear MMSE solution given in [25]. A more detailed accounting can be found in [26]. Let the space of square-integrable r.v.s defined on  $(\Omega, \mathcal{B}, P)$  be denoted as  $L^2(\Omega, \mathcal{A}, P)$ . This is the space of all r.v.s,  $W$ , such that,

$$\|W\|_2 = \int_{\Omega} |W|^2 dP < \infty \quad (3)$$

The linear span of a r.p.,  $X$ , in  $L^2(\Omega, \mathcal{A}, P)$  is the smallest subset of  $L^2(\Omega, \mathcal{A}, P)$  containing  $X$  which possess the properties of a Hilbert space [26] (a subspace). We can define this set by first defining the linear manifold  $L(X_t, t \in T)$  as the set of all r.v.s. with the following form

$$W = \sum_{i=1}^n a_i X_{t_i} \quad a_i \in \mathbb{R}, \quad t_i \in T, \quad n \in \mathbb{N} \quad (4)$$

While  $L(X_t, t \in T)$  is a linear manifold, it is not complete. We can complete this space by including the limits of all Cauchy sequences of elements

in  $L(X_t, t \in T)$ . This complete set is the linear span of a r.p. in  $L^2(\Omega, \mathcal{A}, P)$ , denoted as  $L^2(X)$ . Consider two r.v.s.  $W, V \in L^2(X)$  where  $W = \sum_{t \in T} a_t X_t$ ,  $V = \sum_{s \in T} b_s X_s$ , and  $a_t, b_s \in \mathbb{R}$ . The inner product in  $L^2(X)$  can be written as,

$$\langle W, V \rangle_{L^2} = \mathbb{E}[WV] = \mathbb{E} \left[ \sum_{s, t \in T} a_t b_s X_t X_s \right] = \sum_{s, t \in T} a_t b_s \mathbb{E}[X_t X_s] \quad (5)$$

We can then define the covariance function of the r.p. as

$$R(s, t) = \mathbb{E}[X_t X_s] \quad (6)$$

Then, using equations (5) and (6) we see that the inner product between any two r.v.s in  $L^2(X_t, t \in T)$  can be written in terms of the covariance function of  $\{X_t, t \in T\}$ .

$$\mathbb{E}[WV] = \sum_{s, t \in T} a_t b_s R(s, t) \quad (7)$$

Since the covariance function is a positive semi-definite function, it defines a reproducing kernel, and thus, we can conclude that (7) is an inner product between two elements in the RKHS defined by the autocovariance function ( $\mathcal{H}_R$ ).

$$\langle W, V \rangle_{L^2} = \sum_{s, t \in T} a_t b_s R(s, t) = \langle W', V' \rangle_{\mathcal{H}_R} \quad (8)$$

Equation (8) implies that  $L^2(X)$  and  $\mathcal{H}_R$  are congruent. This means that there exist a congruence mapping, an isomorphism  $\psi(\cdot) : L^2(X) \rightarrow \mathcal{H}_R$ , such that  $\langle W, V \rangle_{L^2(X)} = \langle \psi(W), \psi(V) \rangle_{\mathcal{H}_R}$ . This congruence combined with Riesz Representation Theorem [30] guarantees that any linear functional over  $L^2(X)$  has an exact representation in  $\mathcal{H}_R$ . Therefore, we can define equivalent solutions in either space. Since  $L^2(X)$  contains all possible linear mapping functions over  $X$ , any linear MMSE solution has an exact representation in  $\mathcal{H}_R$ .

Suppose we are given the r.p.  $X$  as input and the r.p.  $Z$  as the desired r.v.. As a consequence of Hilbert projection theorem, the linear MMSE solution can be given as the projection of  $Z$  into  $\mathcal{H}_R$  which is simply the crosscovariance function. This projection is given as,

$$\rho(s) = \mathbb{E}[ZX_s] \quad (9)$$

The MMSE solution is the inner product of  $\rho$  with  $X$  in  $\mathcal{H}_R$  that is

$$Z^* = \langle \rho, X \rangle_{\mathcal{H}_R} = \sum_{s,t \in T} X_t R(s, t)^\dagger \rho(s) \quad (10)$$

Where  $\dagger$  is the Moore-Penrose pseudo inverse. In discrete time, this solution is equivalent to the Wiener solution, where the optimal impulse response is given by  $w^* = \mathbf{R}^\dagger \boldsymbol{\rho}$ , where  $\mathbf{R}$  the auto-covariance matrix and  $\boldsymbol{\rho}$  is the crosscovariance vector. In [25], it is shown in greater detail that the cross-covariance function is the linear MMSE solution in  $\mathcal{H}_R$ . This demonstration shows that with the data-dependent RKHS,  $\mathcal{H}_R$ , there is no need to search for the linear MMSE solution. The solution is the cross-covariance function. The problem is that this solution is still linear in the input space. The natural question that arises is, “can we generalize this idea such that our search space includes nonlinear functions of the input?”. The next section shows the generalization of Parzen’s work in [25].

### 2.3 Nonlinear MMSE Solution

As before, let  $X = \{X_t, t \in T\}$  be a real-valued random process where each  $X_t$  is a r.v. defined on a probability space  $(\Omega, \mathcal{A}, P)$ , and  $T$  is a compact subset of a separable metric space. Let  $\mathcal{F}_\mathcal{X} = \{f_x, x \in \mathcal{X}\}$  be a family of functions  $f_x : \mathbb{R} \mapsto \mathbb{R}$  indexed by the elements of a compact set  $\mathcal{X}$  such that  $\mathbb{E}[|f_x(X_t)|^2] < \infty$  for all  $x \in \mathcal{X}$  and  $t \in T$ . From [26], we have  $L_2(\Omega, \mathcal{A}, P)$  as the Hilbert space of r.v.s in  $(\Omega, \mathcal{A}, P)$  with finite second-order moments. We can define the set  $f(X) = \{f_x(X_t), (x, t) \in \mathcal{X} \times T\}$  as a family of finite second-order random functions indexed by  $x \in \mathcal{X}$  and  $t \in T$ . This set corresponds to the set of all r.v.s that can be written in the form:

$$W = \sum_{i=1}^{n_W} \sum_{j=1}^{m_W} a_{ij} f_{x_i}(X_{t_j}) \quad (11)$$

for some positive integers  $n_W$  and  $m_W$ . From the conditions defined above, we have that  $W \in L^2(\Omega, \mathcal{A}, P)$ . By defining the inner product using the



expected value we can form a linear manifold,  $L(f_x(X_t), (x, t) \in \mathcal{X} \times T)$ ,

$$\begin{aligned} \langle W, V \rangle_{L^2} &= \mathbb{E}[WV] = \sum_{i=1}^{n_W} \sum_{j=1}^{m_W} \sum_{k=1}^{n_V} \sum_{\ell=1}^{m_V} a_{ij} b_{k\ell} \mathbb{E}[f_{x_i}(X_{t_j}) f_{x_k}(X_{t_\ell})] \\ &= \sum_{i=1}^{n_W} \sum_{j=1}^{m_W} \sum_{k=1}^{n_V} \sum_{\ell=1}^{m_V} a_{ij} b_{k\ell} U(t_j, t_\ell, x_i, x_k) \end{aligned} \quad (12)$$

and by completing the space by adding the limits to all Cauchy sequences, we define the Hilbert space  $L^2(f_x(X_t), (x, t) \in \mathcal{X} \times T)$ , or  $L^2(f(X))$  for short. From (12) it is easy to see that for  $s, t \in T$  and  $x, y \in \mathcal{X}$  we can write the function  $U(t, s, x, y)$  as  $U((x, t), (y, s))$ , that is  $U : (\mathcal{X} \times T) \times (\mathcal{X} \times T) \mapsto \mathbb{R}$ , then  $U$  is positive semi-definite.

$$0 \leq \mathbb{E}[|W|^2] = \sum_{i=1}^{n_Y} \sum_{j=1}^{m_Y} \sum_{k=1}^{n_Y} \sum_{\ell=1}^{m_Y} a_{ij} a_{k\ell} U((x_i, t_j), (x_k, t_\ell)) \quad (13)$$

for any  $\mathbf{a} \neq \mathbf{0}$ .

Similar to the linear case, we can write any inner product in  $L^2(f(X))$  as a function of the positive semi-definite function  $U((x_i, t_j), (x_k, t_\ell))$  and vice versa. Therefore, we see that

$$\langle W, V \rangle_{L^2} = \langle W', V' \rangle_{\mathcal{H}_U} \quad (14)$$

where  $W, V \in L^2(f_x(X_t), x, t \in \mathcal{X} \times T)$  and  $W', V' \in \mathcal{H}_U$ .

Equation (14) suggests that  $L^2(f_x(X_t), (x, t) \in \mathcal{X} \times T)$  and  $\mathcal{H}_U$  are congruent. Therefore any MMSE solution in  $L^2(f_x(X_t), (x, t) \in \mathcal{X} \times T)$  has an exact representation in  $\mathcal{H}_U$ , and Parzen's solution in  $\mathcal{H}_U$  is possible.

If we let  $x, y \in \mathcal{X} \subseteq \mathbb{R}$  and  $f_x = \kappa(\cdot, x)$  where  $\kappa(\cdot, \cdot)$  is a reproducing kernel, then  $U((x, t), (y, s)) = \mathbb{E}[\kappa(X_t, x) \kappa(X_s, y)]$ , and the finite second-order moment constraint mentioned above is fulfilled. Therefore, the MMSE solution in  $\mathcal{H}_U$  is the orthogonal projection of some desired r.v.  $Z$  into the space. This function will be a function defined over  $\mathcal{X} \times T$ . The orthogonal projection can be written as,

$$\rho(y, s) = \mathbb{E}[Z f_y(X_s)] = \mathbb{E}[Z \kappa(X_s, y)] \quad (15)$$

Finally, the MMSE solution in  $\mathcal{H}_U$  is

$$\begin{aligned} Z^* &= \langle \rho, X \rangle_{\mathcal{H}_U} = \sum_{s \in T} \sum_{t \in T} \sum_{x \in \mathcal{X}} \sum_{y \in \mathcal{X}} f_x(X_t) U((x, t), (y, s))^\dagger \rho(y, s) \\ &= \sum_{s \in T} \sum_{t \in T} \sum_{x \in \mathcal{X}} \sum_{y \in \mathcal{X}} \kappa(X_t, x) U((x, t), (y, s))^\dagger \rho(y, s) \end{aligned} \quad (16)$$

We refer to this solution in the nonlinear data-dependent RKHS,  $\mathcal{H}_U$ , as the Functional Wiener Filter (FWF).

### 2.3.1 Mercer's theorem and a simple congruence

For the case where we use positive definite kernel  $\kappa$  to define  $f_x := \kappa(\cdot, x)$  with  $x \in \mathcal{X}$ , where  $\mathcal{X}$  is a compact space (for instance a closed interval in  $\mathbb{R}^d$ ), we can define a congruence based on Mercer's theorem. First, note that Mercer's theorem allows us to decompose the kernel as  $\kappa(x, y) = \sum_{m=1}^{N_{\mathcal{H}_\kappa}} \lambda_m \psi_m(x) \psi_m(y)$ , where  $N_{\mathcal{H}_\kappa}$  is either finite or a countable  $\infty$ . Then  $L^2(f(X))$  is congruent with  $L^2(\psi_m(X_t), (t, m) \in T \times \mathbb{N})$  and consequently also congruent with  $\mathcal{H}_U$  where  $U : (T \times \mathbb{N}) \times (T \times \mathbb{N}) \mapsto \mathbb{R}$  is a positive definite kernel defined as:

$$U((t, m), (s, n)) = \mathbb{E}[\psi_m(X_t) \psi_n(X_s)] \quad (17)$$

This additional congruent relationship can be used to change the domain of  $U(s, t, x, y)$  where  $x$  and  $y$  are from a potentially uncountable set, to a countable domain. This is an important step in later sections where we give a method for computing the FWF from realizations.

### 2.3.2 Generalizing $\mathcal{H}_U$

The space of functions we just described corresponds to functions of  $n$  variables that can be expressed as sums of functions on individual variables, that is,

$$g(x_1, x_2, \dots, x_n) = g_1(x_1) + g_2(x_2) + \dots + g_n(x_n), \quad (18)$$

where  $g_i \in \text{span}\{f_x, x \in \mathcal{X}\}$ . Using tap-delay embedding of the random process, we can generalize to functions of vectors in  $\mathbb{R}^D$ . For a random process  $X$  and a given set of relative times  $[\tau_1, \tau_2, \dots, \tau_{D-1}]$ , we can define the tap-delay version  $\mathbf{X}^D = \{\mathbf{X}_t^D, t \in T\}$ , such that  $\mathbf{X}_t^D = [X_t, X_{t-\tau_1}, X_{t-\tau_2}, \dots, X_{t-\tau_{D-1}}]^\top$ . For simplicity, we assume that  $t - \tau_i \in T$  for all  $t \in T$  and all  $i = 1, 2, \dots, D-1$ .

We now proceed just as before by defining the linear manifold  $L(f_x(\mathbf{X}_t^D), (x, t) \in \mathcal{X} \times T)$  as the span of this family, where now  $f_x : \mathbb{R}^D \mapsto \mathbb{R}$ . Any r.v. in this manifold can be written as,

$$W = \sum_{i=1}^{n_W} \sum_{j=1}^{m_W} a_{ij} f_{x_i}(\mathbf{X}_{t_j}^D) \quad (19)$$

Similarly, we denote the completion of this linear manifold by  $L^2(f_x(\mathbf{X}_t^D), (x, t) \in \mathcal{X} \times T)$  or simply as  $L^2(f(\mathbf{X}^D))$ . Furthermore, we can extend the above notation to build nested sets. For example, if  $T$  is the set of integers, we can choose a positive integer  $L > 0$  to build the nested set  $\mathbf{X}_t^{DL} = \{\mathbf{X}_t^D, \mathbf{X}_{t-1}^D, \dots, \mathbf{X}_{t-(L-1)}^D\}$ . We will refer to  $D$  as the sample embedding size, and  $L$  as the window size. By varying  $D$  and  $L$ , the combinations of r.v.s in  $X$  over which the functions in  $\mathcal{H}_U$  are defined can be adjusted.

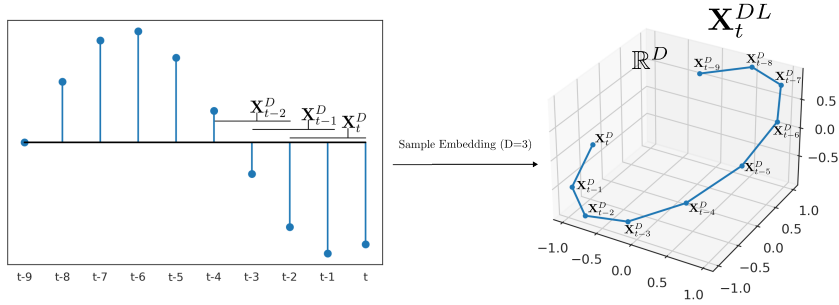


Figure 1: Visual depiction of sample embedding scheme.

These nested sets will give the building blocks for creating a spectrum of spaces with different levels of generality and computation requirements. On one end of this spectrum are less general spaces that will require less computation to compute the MMSE solution and less data for convergence to this MMSE solution. On the other end of this spectrum are more general spaces, which require more computation to compute the MMSE solution and often more data to converge to the MMSE solution. These trade-offs between error, computational complexity, and the necessary amount of training data for convergence are unavoidable and must be balanced via proper selection of the hyperparameters  $L$  and  $D$ . Similar assumptions to those made above are commonplace in KAF, where an “embedding size” is selected that fixes the dimensionality of the inputs [17].

### 3 Computing the MMSE Solution

The sections above show theoretically how to extend Parzen’s idea of a MMSE in a data-dependent universal RKHS. Now we show one method for practically computing the nonlinear MMSE solution. We will begin by

defining an explicit finite-dimensional RKHS that approximates the Gaussian RKHS, and approximate there the solution given in section 2.3.

### 3.1 The Explicit Finite-Dimensional Approximation for the Gaussian RKHS

In [14], an explicit mapping function based on the Taylor expansion of the Gaussian kernel is used to give a finite-dimensional approximation of the feature space specified by the Gaussian kernel. A full derivation of this explicit mapping function can be found in [3]. This is just one way of creating an explicit feature space; another notable technique employs Random Fourier features (RFF) [28], but it has higher computational costs than the Taylor expansion-based method. We will refer to this explicit finite-dimensional Hilbert Space as  $\mathcal{H}_S$ , with kernel  $S(\cdot, \cdot) : \mathbb{R}^D \times \mathbb{R}^D \rightarrow \mathbb{R}$ . The explicit mapping function given in [3] (also see [41]) is written as

$$\phi_{k,j}(x) = e^{-\frac{\|x\|^2}{2\sigma^2}} \frac{1}{\sigma^k \sqrt{k!}} \prod_{i=1}^k x_{j_i} \quad (20)$$

where  $x \in \mathbb{R}^D$ , and  $j \in [D]^k$  enumerates over all selections of  $k$  coordinates of  $x$  (allowing repetitions and enumerating over different orderings of the same coordinates). For instance, the set  $[2]^3$  consists of eight 3-tuples, namely,  $(1, 1, 1)$ ,  $(1, 1, 2)$ ,  $(1, 2, 1)$ ,  $(1, 2, 2)$ ,  $(2, 1, 1)$ ,  $(2, 1, 2)$ ,  $(2, 2, 1)$ , and  $(2, 2, 2)$ . The finite rank approximation of the Gaussian kernel, that is obtained by truncating the Taylor series expansion to the first  $K$  terms,

$$\begin{aligned} S(x, x') &= \langle \phi(x), \phi(x') \rangle_{\mathcal{H}_S} = \sum_{k=0}^K \sum_{j \in [D]^k} \phi_{k,j}(x) \phi_{k,j}(x') \\ &= e^{-\frac{\|x\|^2}{2\sigma^2}} e^{-\frac{\|x'\|^2}{2\sigma^2}} \sum_{k=0}^K \frac{(x^\top x')^k}{\sigma^{2k} k!} = \sum_{m=1}^M \phi_m(x) \phi_m(x') \end{aligned} \quad (21)$$

The last expression in (21) is given by collecting like monomials and flattening  $\phi_{k,j}(x)$  into a vector of size  $M = \binom{D+K}{K}$ , where  $D$  is the dimension of the input vectors and  $K$  is the truncation point. We will use this simplified representation of  $\phi(x) = \{\phi_m(x)\}_{m=1}^M$  from now on.

Since the Gaussian kernel over a closed bounded interval is a Mercer kernel, the representations based on the full Taylor expansion and the eigen-

decomposition of the integral operator induced by the kernel (Mercer's theorem) are equivalent and thus the closure of the span of  $\{\phi_m(X_t), (m, t) \in \mathbb{N} \times T\}$  contains  $L^2(f(X))$ . The truncated series yields a family of functions  $\{\phi_m(X_t), (m, t) \in [1, M] \times T\}$  where we can approximate any  $f_x = G_\sigma(\cdot, x)$  by a finite superposition:

$$f_x(x') \approx \sum_{m=1}^M \phi_m(x) \phi_m(x'), \quad (22)$$

Due to the exponential decay of the Gaussian kernel's eigenvalues, effective finite-rank approximations can often be obtained with just a few features in the expansion [14]. The main advantage of the explicit feature space in the context of this work is that it simplifies the design of linear operators in the feature space because we can represent them as finite-dimensional matrices. Also, since operators can be represented as matrices and functionals as vectors, computations in  $\mathcal{H}_S$  enjoy the computational tractability of matrix and vector multiplications.

We should draw attention to some deficiencies of this finite-dimensional RKHS. In [34], an overview of universal and characteristic reproducing kernels is given. A reproducing kernel is c-universal if any target function can be approximated to an arbitrary degree of accuracy, provided the search algorithm converges to the desired function and the number of training samples goes to infinity. A reproducing kernel is called characteristic if the kernel mean embedding is an injective function. In [22] it is shown that a kernel is c-universal if and only if it is characteristic. The Gaussian kernel is both c-universal and characteristic. However, its finite approximation,  $S(\cdot, \cdot)$ , loses these properties. As an example, consider two probability measures say  $p(x)$  and  $q(x)$  whose kernel mean embeddings using the Gaussian kernel have feature space representations,  $\{\phi_n(p(x))\}_{n=1}^\infty$  and  $\{\phi_n(q(x))\}_{n=1}^\infty$ . There may be pairs of probability measures such that

$$\phi_n(p(x)) = \phi_n(q(x)) \quad \forall n \leq k, \quad \phi_n(p(x)) \neq \phi_n(q(x)) \quad \forall n > k \quad (23)$$

Since  $S(\cdot, \cdot)$  is a truncation of this feature space, two probability measures satisfying (23) cannot be disambiguated in  $\mathcal{H}_S$  and therefore the mean embedding in  $\mathcal{H}_S$  is not injective. This also means that  $\mathcal{H}_S$  is not universal. While these issues are theoretically consequential, due to the eigenvalue roll-off of the Gaussian kernel, we expect that the effects of this deficiency of

$\mathcal{H}_S$  will be manageable. This assumption will be experimentally validated in later sections.

In previous works such as [14], [28], and [41], an explicit mapping function is used to decouple model size from the number of training samples. While our method inherits this as a strength of using an explicit approximation, we will also see that it is necessary to work with individual features of the RKHS if we want to define a closed-form MMSE solution that is practically computable. Therefore, the explicit RKHS provides an elegant and efficient way of performing the operations necessary for our closed-form solution.

### 3.2 Covariance kernel for the approximate MMSE Solution with the explicit feature map

The solution in section 2.3 requires the definition of a family of r.v.s. with finite second-order moments. Our truncated approximation that computes an explicit feature map provide us with an alternative family of r.v.s  $\{\phi_m(\mathbf{X}_t^D), (m, t) \in \mathbb{N} \times T\}$ , abbreviated as  $\phi(\mathbf{X}^D)$  as our family of functions with finite second-order moments. Next, we will show how to compute the covariance kernel,  $\mathbf{U}(s, t, m, n)$ , and define the inner product in  $\mathcal{H}_U$ . Then we will show how to compute the projection of some desired r.v. into  $\mathcal{H}_U$  giving the nonlinear MMSE solution.

With our family of functions  $\phi(\mathbf{X}^D)$ , the covariance kernel  $\mathbf{U}$  is given as,

$$\mathbf{U}(t, s, m, n) = \mathbb{E}[\phi_m(\mathbf{X}_t^D)\phi_n(\mathbf{X}_s^D)] \quad t, s \in T \quad m, n \in [1, M] \quad (24)$$

Then, we can approximate random variables in  $L^2(\phi(\mathbf{X}^D))$  as defined in (19), as follows:

$$\begin{aligned} W &\approx \sum_{q=1}^{m_W} \sum_{m=1}^M \sum_{i=1}^{n_W} a_{iq} \phi_m(x_i) \phi_m(\mathbf{X}_{t_q}^D) = \sum_{q=1}^{m_W} \sum_{m=1}^M A_{q,m} \phi_m(\mathbf{X}_{t_q}^D) \\ A_{q,m} &= \sum_{i=1}^{n_W} a_{iq} \phi_m(x_i) \end{aligned} \quad (25)$$

With inner product given by:

$$\begin{aligned}
\langle W, V \rangle_{L^2} &= \mathbb{E}[WV] = \sum_{q=1}^{m_W} \sum_{m=1}^M \sum_{p=1}^{m_V} \sum_{n=1}^M A_{q,m} B_{p,n} \mathbb{E}[\phi_m(X_{t_q}) \phi_n(X_{t_p})] \\
&= \sum_{q=1}^{m_W} \sum_{m=1}^M \sum_{p=1}^{m_V} \sum_{n=1}^M A_{q,m} B_{p,n} \mathbf{U}(t_q, t_p, m, n)
\end{aligned} \tag{26}$$

Assuming strict stationarity of  $X$ , we have that  $\mathbf{U}(t, s, m, n) = \mathbf{U}(t - \tau, s - \tau, m, n)$ . If we pick a set of  $L$  relative times to  $t \in T$ , the joint statistics of the set of random vectors  $[\mathbf{X}_t^D, \mathbf{X}_{t-1}^D, \dots, \mathbf{X}_{t-(L-1)}^D]$  are the same as  $[\mathbf{X}_s^D, \mathbf{X}_{s-1}^D, \dots, \mathbf{X}_{s-(L-1)}^D]$ . Then we can represent the relative time information along with the feature index as a matrix  $\mathbf{U} \in \mathbb{R}^{(M \cdot L) \times (M \cdot L)}$ . The details of exactly how to construct this matrix and its relation to  $U(s, t, x, y)$  are given in A.

Finally, we can define the projection of a desired r.v.  $Z$  into  $\mathcal{H}_U$  using the crosscovariance function.

$$\tilde{\rho}(t, m) = \mathbb{E}[Z \phi_m(\mathbf{X}_t^D)] \tag{27}$$

The feature space representation of this function can be given as,

$$\boldsymbol{\rho} = \mathbb{E}[Z \phi(\mathbf{X}_t^{DL})] \quad \phi(\mathbf{X}_t^{DL}) := \begin{bmatrix} \phi(\mathbf{X}_t^D) \\ \vdots \\ \phi(\mathbf{X}_{t-(L-1)}^D) \end{bmatrix} \in \mathbb{R}^{M \cdot L}. \tag{28}$$

where

Then the MMSE in  $\mathcal{H}_U$  is

$$\hat{Z} = \phi(\mathbf{X}_t^{DL})^\top \mathbf{U}^\dagger \boldsymbol{\rho} \tag{29}$$

Notice that this equation has the same form as the linear MMSE solution given in equation (10) except that the number of dimensions is larger for the nonlinear case. While the number of dimensions in the linear MMSE solution is related only to time, the number of dimensions in the nonlinear solution is related to both time and feature space index as a result of the RKHS we employ (see Table 1 for a comparison between all spaces introduced here).

RKHS	Domain of Kernel Function	Nonlinear	Data-dependent	Includes Notion of Time
$\mathcal{H}_R$	$T \times T$		✓	✓
$\mathcal{H}_\kappa$	$\mathbb{R}^D \times \mathbb{R}^D$	✓		
$\mathcal{H}_S$	$\mathbb{R}^D \times \mathbb{R}^D$	✓		
$\mathcal{H}_U$	$(\mathbb{R}^D \times T) \times (\mathbb{R}^D \times T)$	✓	✓	✓
$\mathcal{H}_U$	$(\mathbb{N} \times T) \times (\mathbb{N} \times T)$	✓	✓	✓

Table 1: Brief description of the different RKHSs used so far.

### 3.3 Error Analysis

Now we will discuss some sources of error in the FWF solution. First, it is essential to remember that we can only calculate the FWF solution in a finite-dimensional RKHS, therefore  $\mathcal{H}_S$ , and transitively  $\mathcal{H}_U$ , can only be universal if  $K$  approaches infinity and  $D$  approaches the true model order. This deficiency of  $\mathcal{H}_U$  can be a source of error. In [3], error bounds for the approximation made by  $S(\cdot, \cdot)$  to the universal Gaussian kernel are given. Second, we still need to select the Gaussian kernel size, which in the FWF only affects the precision of the results for finite training datasets. Third, since we are quantifying the joint distribution between pairs of samples projected into an RKHS and taking their mean, implicitly, we are assuming that the system we are modeling is strictly stationary. Any deviation from this stationary assumption can cause error. Fourth, there can be numerical error associated with the conditioning of the  $\mathbf{U}$  matrix.

In [25] a theoretical MMSE for the solution in  $\mathcal{H}_R$  is given with the equation

$$\mathbb{E}[|Z - \mathbb{E}[Z|L^2(X)]|^2] = \mathbb{E}[|Z|^2] - \langle \rho, \rho \rangle_{\mathcal{H}_R}. \quad (30)$$

We can extend this theoretical MMSE to  $\mathcal{H}_U$  by measuring the distance between the projection of  $Z$  into  $\mathcal{H}_U$  and  $Z$  in a similar manner to equation (30).

$$\mathbb{E}[|Z - \mathbb{E}[Z|L^2(\phi(\mathbf{X}^D))]|^2] = \mathbb{E}[|Z|^2] - \langle \tilde{\rho}, \tilde{\rho} \rangle_{\mathcal{H}_U}. \quad (31)$$

This equation gives the MMSE for the solution in the finite-dimensional RKHS,  $\mathcal{H}_U$ . Since the projection of  $Z$  in  $\mathcal{H}_U$  is orthogonal, the difference between the power of the desired response and the norm squared of its projection in  $\mathcal{H}_U$  is the expected MSE. Therefore, it is quite easy to select the hyper parameters of the modeling ( $M$ ,  $L$  and kernel size) to achieve the desired error. This is markedly different from KAF and other filtering methods, where we have to evaluate the MSE on the training set by directly comparing



model outputs with desired responses for different hyperparameters. Therefore, discounting numerical error, we can say that all the sources of error mentioned above are combined in the inner product calculation of the space  $\mathcal{H}_U$ .

Figure 2 shows the theoretical MMSE, the absolute difference between theoretical and calculated MSE in the training set, and the test set MSE as a function of the FWF hyperparameters for prediction on the nonlinear chaotic Mackey-Glass time series with a kernel size of 0.25. As can be expected the larger the number of lags and dimension of the explicit RKHS, the smaller the error. This figure also shows that the training set MSE follows the theoretical error almost exactly for a large range of hyperparameter values. Figure 2 also shows the test set MSE as a function of  $M$  and  $L$ . We can observe that the test set performance largely follows the training MSE, but for large delays and number of eigenfunctions flattens, which is explained by over-fitting. Since the FWF is a linear model, techniques for model order estimation [35] can be applied to improve generalization, but we leave this to future work.

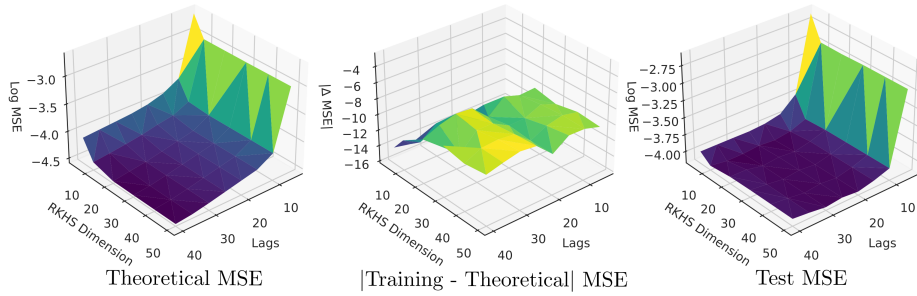


Figure 2: |Training - Theoretical| MSE in log scale (middle), Theoretical MSE (left), and Test MSE (right) as a function of  $K$  and  $L$  for prediction of Mackey-Glass time series.

### 3.4 The Functional Wiener Equation

Thus far, we have given the solution for a nonlinear MMSE filter in  $\mathcal{H}_U$  by extending Parzen's ideas. It is interesting to see the ramifications of this formulation on the system of equations solved by the linear Wiener Filter.

To this end, we will now develop an analog to this system of equations, which describes the problem we implicitly solve with the Functional Wiener Filter.

In this discussion, we will assume that the kernel-based integral operators in question are Hilbert-Schmidt. We start by examining the operator related to the kernel  $U$ . An operator over a Hilbert space can be represented as an integral operator defined by its corresponding kernel function. This representation is coordinate-free. Alternatively, a matrix with dimensions equal to the number of dimensions in the Hilbert Space can be used, here the values in this matrix depend on some chosen coordinate system. In this work, the  $\mathbf{U}$  matrix is a matrix representation of an operator with respect to the coordinate system(feature space) of  $\mathcal{H}_S^L$ . Using the relationship between  $\mathbf{U}$  and  $U(s, t, m, n)$  given in Appendix A we can recover an operator over  $\mathcal{H}_S$  for each pair of time indices  $s, t$

$$U(s, t, x, y) \approx \sum_{n=1}^M \sum_{m=1}^M \mathbf{U}(t, s, n, m) \phi_n(x) \phi_m(y) \quad (32)$$

where  $x, y \in \mathcal{X} \subset \mathbb{R}^D$ , for specific values of  $s, t \in T$  and  $n, m \in [1, M]$ . We can think of  $U(s, t, x, y)$  as a collection of operators over functions of the RKHS  $\mathcal{H}_\kappa$  induced by the kernel  $\kappa$ , indexed with pairs of indices  $(s, t)$ . Alternatively, when we only consider  $L$  relative times, we could view  $U(s, t, x, y)$  as a single operator over  $\mathcal{H}_\kappa^L$ . The equation implicitly solved in (29) can then be given as

$$\sum_{t=0}^{L-1} \left[ \int_{\mathcal{X}} w(t, x) U(s, t, x, y) dx \right] = \rho(s, y) \quad (33)$$

where  $w, \rho \in \mathcal{H}_\kappa^L$ . Note that  $\rho(s, y)$  is the crosscovariance function defined in (15).

When we approximate  $U$  based on the truncated kernel  $S$  which is represented by the matrix  $\mathbf{U}$  and multiply this by the vector  $\boldsymbol{\rho}$  we solve for  $\mathbf{w}^* = \mathbf{U}^\dagger \boldsymbol{\rho}$ , which is the vector approximation of the function,  $w^*(t, x)$  that solves (33). Equation (33) is a direct nonlinear analog to the system of equations solved by the linear Wiener Filter in discrete time. For this reason, we call it the Functional Wiener Filter equation.

In principle, the extension of equation (33) for continuous time can be written as,

$$\int_a^b \left[ \int_{\mathcal{X}} w(t, x) U(s, t, x, y) dx \right] dt = \rho(s, y) \quad (34)$$

where  $a \leq s \leq b$ . However, the techniques detailed in section 3.2 do not extend to the continuous time operator.

### 3.5 The Functional Wiener Filter as a Difference Equation

Similar to the linear Wiener Filter, the Functional Wiener Filter can be interpreted as the optimal solution under the assumption of a difference equation with a specific form. In the linear case this difference equation corresponds to an FIR linear filter, with the form

$$\hat{z}_t = \sum_{\tau=0}^{L-1} w_\tau x_{t-\tau} \quad w_\tau, x_{t-\tau} \in \mathbb{R} \quad (35)$$

In the case of the Functional Wiener Filter we replace scalar multiplication with nonlinear functions. Due to sample embeddings, these nonlinear functions may be defined over multiple samples rather than single samples.

$$\hat{z}_t = \sum_{\tau=0}^{L-1} f_\tau(\mathbf{x}_{t-\tau}^D) \quad f_\tau \in \mathcal{H}_S, \mathbf{x}_t^D \in \mathbb{R}^D \quad (36)$$

The easiest way to explain how the FWF defines a difference equation is by first calculating,

$$\mathbf{w}^* = \mathbf{U}^\dagger \boldsymbol{\rho} \quad (37)$$

Then the FWF solution can be written as,

$$Z_t = \phi(\mathbf{X}_t^{DL})^\top \mathbf{U} \boldsymbol{\rho} = \phi(\mathbf{X}_t^{DL})^\top \mathbf{w}^* \quad (38)$$

The rightmost expression in equation 38 can be written as,

$$\hat{z}_t = \phi(\mathbf{x}_t^{DL})^\top \mathbf{w}^* = \sum_{\tau=0}^{L-1} \phi(\mathbf{x}_{t-\tau}^D)^\top \mathbf{w}_{M\tau:(M\tau)+(M-1)}^* = \sum_{\tau=0}^{L-1} f_\tau^*(\mathbf{x}_t^D) \quad (39)$$

Therefore the subvectors  $\mathbf{w}_{M\tau:(M\tau)+(M-1)}^*$  are the feature space representations of  $f_\tau^*$ .

Note that  $\mathcal{H}_S$  becomes universal on  $\mathbb{R}^D$  when  $K$  goes to infinity. Every solution found using the Functional Wiener Filter follows this form. This highlights a distinction between the FWF and other KAF methods found in

[16], [15], [6], and [17]. The FWF is defined over  $\mathbb{R}^D \times T$  (time and space) rather than just over  $\mathbb{R}^D$ . The interpretation of the FWF as a nonlinear difference equation gives a clearer picture of what the FWF learns and can provide insight into the dynamics of the model that generates the input time series and the failure states of the learned models. In the experimental section, we will demonstrate how this interpretation can be used to extract a difference equation from data. Note that this type of interpretation is not possible with any other KAF method mentioned above.

## 4 Experiments

We will compare the FWF solution derived above in two important applications: nonlinear mapping of one time series into another (as required in system identification) and nonlinear time series prediction. The models used for comparison are the linear Wiener Filter (WF) [38], Gaussian Process Regression (GPR) [40], Kernel Least-Mean Squares (KLMS) [16], Extended Kernel Recursive Least-Squares (KRLS) [15], Kernel Ridge Regression (KRR) [10], and Augmented Space Linear Model (ASLM) [27], which is a linear model in the joint space of the data and desired response, improving slightly the performance of the Wiener solution. The error bars in figures 4,5,6 represent the range of test MSE(i.e. they show the worst test MSE and best test MSE).

Method	Training	Evaluation
FWF	$\mathcal{O}(M^2 L^2 N) + \mathcal{O}(M^3 L^3)$	$\mathcal{O}(ML)$
KLMS	$\mathcal{O}(N)$	$\mathcal{O}(N)$
KRLS	$\mathcal{O}(N^2)$	$\mathcal{O}(N)$
ASLM	$\mathcal{O}(L^2 N)$	$\mathcal{O}(L) + \mathcal{O}(\log(N))$
KRR	$\mathcal{O}(N^3)$	$\mathcal{O}(N)$
GPR	$\mathcal{O}(N^3)$	$\mathcal{O}(N)$
WF	$\mathcal{O}(L^2 N)$	$\mathcal{O}(L)$

Table 2: Computational Complexity Comparison for both training and evaluation:  $M = \binom{D+K}{K}$  (number of dimension in  $\mathcal{H}_S$ ),  $N$  (number of training samples),  $L$  (window size)

Table 2 shows a comparison of the computational complexity between the different methods. Since the FWF utilizes the explicit finite-dimensional RKHS, the computation cost of evaluating the model is decoupled from the

number of training samples used, as in the Wiener filter. The hyperparameters that affect the computational complexity of the FWF are  $D$ ,  $K$ , and  $L$ , and if  $N \gg ML$ , then the  $\mathcal{O}(M^2 L^2 N)$  will dominate the training complexity. Note that the use of sample embeddings will increase the number of dimensions in  $\mathcal{H}_S$ ; therefore, this generalization does not come without additional computational cost.

For each experiment, a grid search across the hyperparameters of each model was performed. However, for brevity, we give the finer details of the other searches in the supplementary materials.

#### 4.1 Demonstration of the Difference Equation Interpretation

We will now use the interpretation given in section 3.5 to discover the underlying functions that generate a time series. First, we will discuss the system used in this experiment. The input r.p.,  $X$ , is white Gaussian noise drawn from the distribution  $\mathcal{N}(0, \pi)$ . The model output,  $Z$ , is created by applying the nonlinear mapping given in (40) to  $X$ .

$$\begin{aligned} Z_t = & 0.5 \tanh(X_t)^2 + \sin(X_{t-1})^3 + 0.5 \tanh(X_{t-2})^3 \\ & + 0.2 \sin(X_{t-3})^2 + 0.75 \tanh(X_{t-4})^2 \end{aligned} \quad (40)$$

The FWF is then tasked with finding a mapping function from  $X$  to  $Z$  i.e., a conventional system identification setting. The bottom half of figure 3 shows the  $L$  functions (one for each value of  $\tau$ ) found by the FWF. The green histograms show the p.d.f of the realizations used in the training set, scaled for visualization. We observe that in regions covered in the training set, the functions learned by the FWF are vertically shifted (biased) versions of the true functions given in equation (40). However, when these biased versions are summed together, they converge to the true difference equation given in (40). Centering the covariance in RKHS will compensate for the bias. It's also interesting that the FWF outputs are constant for values of  $\tau$  which are larger than the true memory depth of the system.

The top right plot in Figure 3 compares the performance of the FWF with the other nonlinear filtering methods mentioned above. Each method was tested with 5 different training and testing windows at each value of  $N$ . The average test set MSE is shown with error bars, giving the variance of

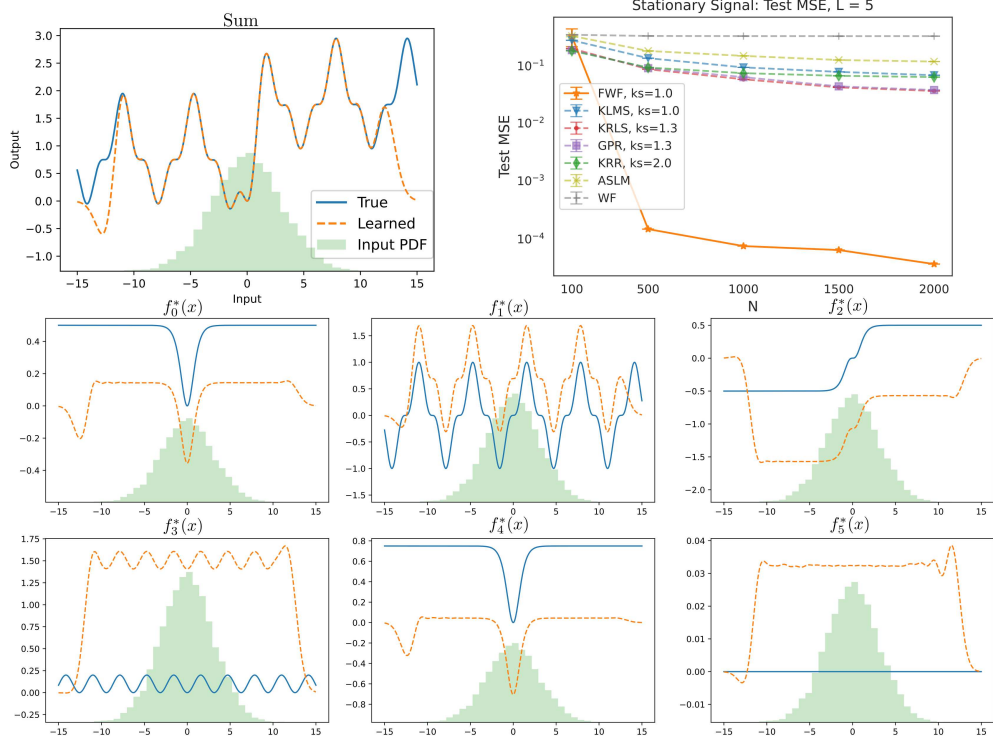


Figure 3: Visualization of the underlying functions learned by the FWF on the strictly stationary task (bottom) and their sum (top left). Comparison of test set MSE as a function of the number of training samples ( $N$ ). (top right).  $ks$  is the kernel size used for each method.

the test set MSE across the different training and testing windows. For each method, a search across a range of kernel sizes (0.75 – 2 at increments of 0.1) was performed, and the best results for each method are shown. The FWF provides a clear performance boost over the other methods on this task. This suggests that if the model assumptions hold, then its performance is better than the other nonlinear filtering methods. Moreover, we can plot the underlying functions learned by the FWF at each lag and can interpret the results as a difference equation.

## 4.2 Mackey-Glass Prediction

The Mackey-Glass is a chaotic nonlinear time series with equation

$$\frac{dx_t}{dt} = \frac{a\theta^n x_{t-\tau}}{\theta^n + x_{t-\tau}^n} - bx_t \quad (41)$$

This time series was introduced in [21] as a model capable of producing nonlinear chaotic behavior similar to respiratory and hematopoietic diseases. It is commonly used to test time series prediction methods (see [7, 19, 17]). In this experiment we use the values  $a = 0.2$ ,  $b = 0.1$ ,  $n = 10$ ,  $\theta = 1$  and  $\tau = 30$ . The time series is then discretized with a sampling period of 6 seconds.

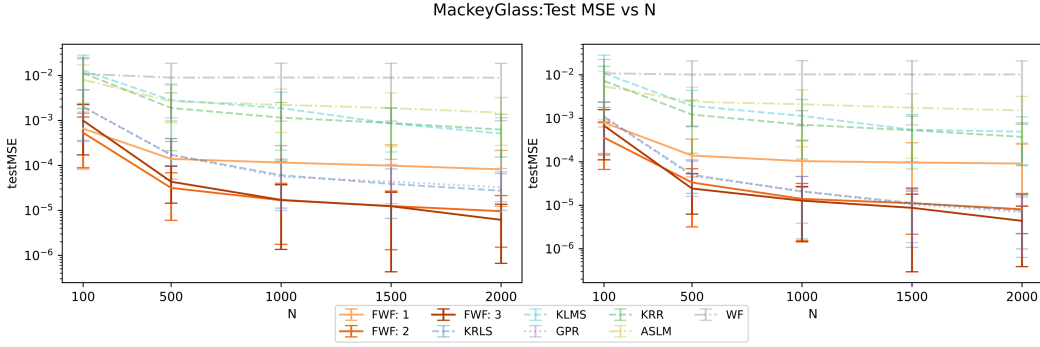


Figure 4: Comparison of Test MSE on Mackey-Glass task window sizes of  $L = 20$ (left) and  $L = 15$ (right).

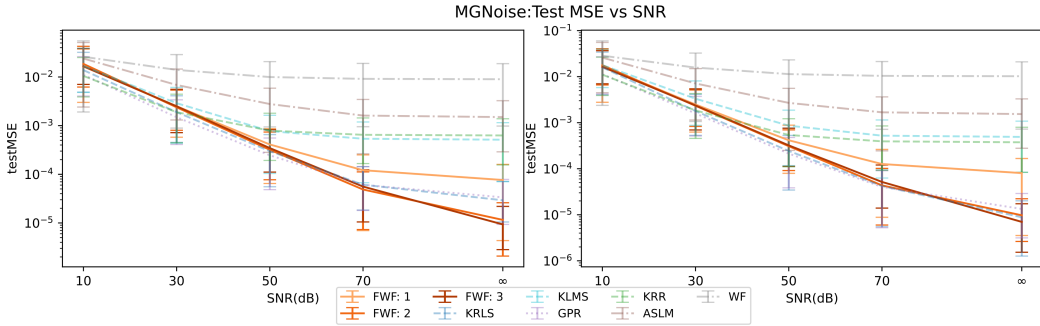


Figure 5: Comparison of Test MSE on noisy Mackey-Glass with window sizes of  $L = 20$ (left) and  $L = 15$ (right),  $N = 2000$  for all noise levels.

A Gaussian kernel was used for all kernel methods. Figure 4 shows the test set MSE as a function of the number of training samples ( $N$ ) for window sizes ( $L$ ) of 15 and 20. For each value of  $N$  we use 5 different training windows and take the average test MSE across these trials. We perform a hyperparameter search for each method and show the best MSE for each method in Figure 4. We tested the FWF with sample embedding sizes ( $D$ ) of 1, 2, and 3. For FWF with sample embeddings of 2 and 3, we use a truncation point ( $K$ ) of 10. For the FWF with  $D = 1$ , we use a truncation point of 25. Larger values of  $K$  were tested, but did not improve performance. For this task, increasing  $D$  improves the performance of the FWF markedly. When compared to the other kernel methods, the FWF with  $D = 2, 3$  is on par with KRLS and GPR for  $L = 15$ , and outperforms KRLS and GPR for  $L = 20$ . For the FWF with  $D = 1$ , the MSE flattens at 500 training samples. For the FWF with  $D = 2, 3$  more samples are needed for the MSE curve to flatten, which supports our claim of the trade-off between more general spaces and the amount of data necessary to estimate the MMSE solution.

We also tested robustness to input noise by adding white Gaussian noise at increasing levels to the input of the model. Figure 5 shows the performance for each method for a given signal-to-noise ratio. The same hyperparameter search done for the noiseless prediction case was used. We see that the FWF exhibits similar sensitivity to noise as the other methods.

### 4.3 Lorenz Attractor

The Lorenz attractor, introduced in [20], is a three-dimensional system of equations that can exhibit chaotic behavior.

$$\frac{dx}{dt} = \sigma(y - x), \quad \frac{dy}{dt} = x(\rho - z) - y, \quad \frac{dz}{dt} = xy - \beta z \quad (42)$$

The Lorenz system is commonly used to test time series prediction and forecasting models (see [32], [15], and [2]). For this experiment, the parameters  $\sigma$ ,  $\rho$ , and  $\beta$  are set to 10, 28, and  $\frac{8}{3}$  respectively. The models are given the  $x$ -component of this system as input. The desired time series is the  $z$ -component of the Lorenz attractor five samples in the future. Each method is tested on five different training and testing windows for each value of  $N$ . As before, we perform a grid search (0.5 – 2 in increments of 0.25) for the best kernel size for each method. Figure 6 shows that the FWF with  $D = 3$



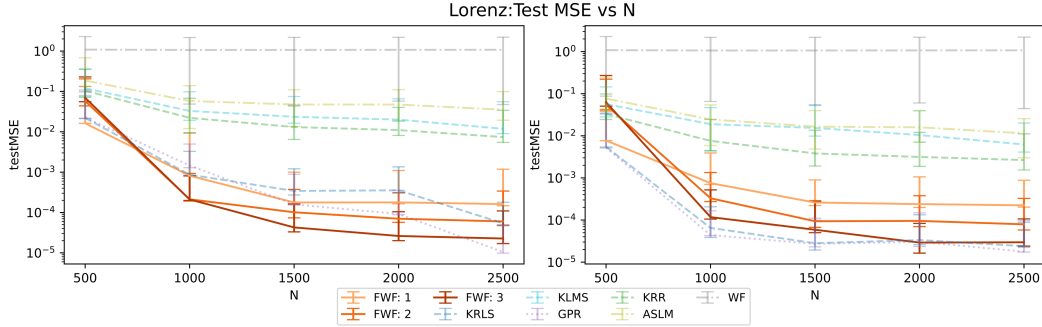


Figure 6: Comparison of Test MSE on Lorenz task with window sizes of  $L = 20$ (left) and  $L = 15$ (right).

is as performant as KRLS and GPR for this task. The FWF again improves in performance with an increase in  $D$ .

#### 4.4 SunSpot

In this experiment, we test the methods on a real-world dataset (measured rather than simulated), the sunspot data [8]. This time series contains monthly averages of the daily sunspot numbers reported from the WDC-SILSO, Royal Observatory of Belgium. The time series is standardized to have zero mean and a standard deviation of 1. The task for the models is to forecast the number of sunspots 10 samples in the future. A grid search ( $0.75 - 3$  in increments of  $0.25$ ) for the best kernel size for each kernel method was performed. The number of training samples is 2000 and the test set is 300 samples. The average MSE and standard deviation for the best set of hyperparameters across 5 different training windows are given in 3.  $L = 10$  for all methods. On this task, the FWF with  $D = 2$  performs best in the test set.

Method	Train MSE	Test MSE
FWF( $D = 1$ )	$0.306 \pm 0.0059$	$0.354 \pm 0.0080$
FWF( $D = 2$ )	$0.168 \pm 0.0016$	<b><math>0.182 \pm 0.0089</math></b>
FWF( $D = 3$ )	$0.122 \pm 0.0014$	$0.213 \pm 0.02$
KRLS	$0.27 \pm 0.0012$	$0.323 \pm 0.0072$
KLMS	$0.366 \pm 0.0017$	$0.374 \pm 0.0069$
GPR	$0.279 \pm 0.0012$	$0.324 \pm 0.0061$
KRR	$0.282 \pm 0.0011$	$0.326 \pm 0.0054$
ASLM	$0 \pm 0$	$0.568 \pm 0.0093$
WF	$0.33 \pm 0.0007$	$0.382 \pm 0.0047$

Table 3: Train and Test MSE for Sunspot forecasting on the normalized data.

## 5 Conclusions

In summary, we have successfully extended Parzen’s MMSE in  $\mathcal{H}_R$ , to a nonlinear data-dependent RKHS,  $\mathcal{H}_U$ . In  $\mathcal{H}_U$ , the MMSE solution can be expressed as the cross-covariance function. Essentially, when the statistics of the input r.p. are embedded into the inner product of a space, the orthogonal projection of any desired r.v. (i.e. the MMSE solution) is immediately given by the cross-covariance function.

The calculation of the nonlinear MMSE solution is simplified with the use of an explicit finite-dimensional RKHS that approximates the universal Gaussian kernel. In this finite-dimensional space, the  $U$  operator takes the form of a finite-dimensional matrix, which is used to define the inner product in  $\mathcal{H}_U$ . This is a strength of using a finite-dimensional RKHS, as it greatly simplifies the calculation of inner products in  $\mathcal{H}_U$ .

Although the FWF belongs to the KAF family, its principles are different and represent a fresh approach to exploit the linear structure of the Hilbert space. Rather than implementing search techniques in a data-independent space, we focus on first building the RKHS in which we define our solution. Then show that search is not necessary in this space. Another distinction between FWF and other KAF is that the FWF solution defines functionals over time and space (i.e. the amplitude values of the signal).

In future work, we should address some practical limitations of the method. One of these limitations is that the dimensionality of  $\mathcal{H}_U$  grows exponentially with sample embedding size. Other methods for explicit space approximations, which are more efficient in terms of dimensionality, are needed. We

should also further investigate how sensitive the solution is to data non-stationarity and seek methods for lifting this assumption. We should also expand on the interpretation of the FWF as a nonlinear difference equation and see what sorts of insights can be gained from this interpretation. Finally, one deeper question stemming from this work is: Can we define a practical technique for taking inner products in  $\mathcal{H}_U$  without first referencing an extrinsic coordinate system? Answering this question would yield a completely data-determined Hilbert space which is truly the “natural” setting for taking conditional expectations with respect to  $X$ .

## A The $\mathbf{U}$ matrix

In section 3.2 an abbreviated construction of the  $\mathbf{U}$  matrix is given. Here we show a more explicit construction of this matrix as a block matrix. Due to strict stationarity, we can remove the dependence on  $s, t$  and let  $s = t - \tau$ . Then

$$\mathbf{U}(\tau, n, m) = \mathbb{E}[\phi_n(\mathbf{X}_t^D)\phi_m(\mathbf{X}_{t-\tau}^D)] \quad (43)$$

Intuitively,  $\mathbf{U}(\tau, n, m)$  measures the correlation between the projection of  $\mathbf{X}_t^D$  and  $\mathbf{X}_{t-\tau}^D$  across all dimensions of  $\mathcal{H}_S$ . For each value of  $\tau = 0, 1, \dots, L-1$ , we will get a  $M \times M$  dimensional matrix,

$$\mathbf{U}_\tau = \begin{bmatrix} \mathbf{U}(\tau, 1, 1) & \dots & \dots & \mathbf{U}(\tau, 1, M) \\ \vdots & \ddots & \dots & \vdots \\ \mathbf{U}(\tau, M, 1) & \dots & \dots & \mathbf{U}(\tau, M, M) \end{bmatrix} = \mathbb{E}[\phi(\mathbf{X}_t^D)\phi(\mathbf{X}_{t-\tau}^D)^\top] \quad (44)$$

Under the assumption of finite model order, the matrix  $\mathbf{U}$  is a  $((M \cdot L) \times (M \cdot L))$  dimensional positive semi-definite matrix,

$$\mathbf{U} = \begin{bmatrix} \mathbf{U}_0 & \mathbf{U}_1 & \dots & \mathbf{U}_{L-1} \\ \mathbf{U}_1^\top & \mathbf{U}_0 & \dots & \mathbf{U}_{L-2}^\top \\ \vdots & \vdots & \ddots & \vdots \\ \mathbf{U}_{L-1}^\top & \mathbf{U}_{L-2}^\top & \dots & \mathbf{U}_0 \end{bmatrix} \quad (45)$$

Since  $\mathbf{U}$  is the covariance matrix of  $\phi(\mathbf{X}_t^{DL})$  (the same for all  $t$  because of stationarity), it is a positive semi-definite matrix [24]. The  $\mathbf{U}$  matrix describes the correlations of the projection of  $\mathbf{X}^{DL}$  across both space (the features of  $\mathcal{H}_S$ ) and time.

Now we show exactly how  $\mathbf{U}$  is related to  $U(s, t, x, y)$ . Assuming strict stationarity,  $U(s, t, x, y)$  can be written as a function of  $\tau = |s - t|$ . The following relationship between the submatrices of  $\mathbf{U}$  and  $U(\tau, x, y)$  is given as,

$$U(\tau, x, y) \approx \sum_{n=1}^M \sum_{m=1}^M \mathbf{U}(\tau, n, m) \phi_n(x) \phi_m(y) \quad (46)$$

where  $\mathbf{U}(\tau, n, m)$  is defined in equation (43). A simulation that empirically validates 46 is given in the supplementary materials.

## Funding

This material is based upon work supported by the Office of the Under Secretary of Defense for Research and Engineering under award number FA9550-21-1-0227, and partially supported by ONR grants N00014-21-1-2295 and N00014-21-1-2345. This research was supported by the Science, Mathematics and Research for Transformation (SMART) Scholarship Program.

## References

- [1] Badong Chen et al. “Quantized Kernel Least Mean Square Algorithm”. In: *IEEE Transactions on Neural Networks and Learning Systems* 23.1 (2012), pp. 22–32.
- [2] Y. Chen, Y. Qian, and X. Cui. “Time series reconstructing using calibrated reservoir computing”. In: *Sci Rep* 12, 16318 (2022) (2002).
- [3] Andrew Cotter, Joseph Keshet, and Nathan Srebro. *Explicit Approximations of the Gaussian Kernel*. 2011. arXiv: 1109.4603 [cs.AI].
- [4] D. Duttweiler and T. Kailath. “An RKHS approach to detection and estimation problems–IV: Non-Gaussian detection”. In: *IEEE Transactions on Information Theory* 19.1 (1973), pp. 19–28.
- [5] D. Duttweiler and T. Kailath. “An RKHS approach to detection and estimation problems–V: Parameter estimation”. In: *IEEE Transactions on Information Theory* 19.1 (1973), pp. 29–37.
- [6] Y. Engel, S. Mannor, and R. Meir. “The kernel recursive least-squares algorithm”. In: *IEEE Transactions on Signal Processing* 52.8 (2004).

- [7] Mohammad Farzad, Hanif Tahersima, and Hamid Khaloozadeh. “Predicting the Mackey Glass Chaotic Time Series Using Genetic Algorithm”. In: *2006 SICE-ICASE International Joint Conference*. 2006, pp. 5460–5463.
- [8] David Hathaway. *Sun Spot Numbers*. URL: <https://solarscience.msfc.nasa.gov/SunspotCycle.shtml>. accessed: 08/02/2024.
- [9] Takeyuki Hida and Nobuyuki Ikeda. “Analysis on Hilbert Space with Reproducing Kernel Arising from Multiple Wiener Integral”. In: *Selected Papers of Takeyuki Hida*. World Scientific, 1967, pp. 142–168.
- [10] Arthur E. Hoerl and Robert W. Kennard. “Ridge Regression: Biased Estimation for Nonorthogonal Problems”. In: *Technometrics* 42.1 (2000), pp. 80–86. ISSN: 00401706. (Visited on 09/05/2023).
- [11] T Kailath and D Duttweiler. “An RKHS approach to detection and estimation problems-part III: Generalized innovations representations and a likelihood-ratio formula”. In: *IEEE Trans. Inf. Theory* 18.6 (1972), pp. 730–745.
- [12] T Kailath and H Weinert. “An RKHS approach to detection and estimation problems-part II: Gaussian signal detection”. In: *IEEE Trans. Inf. Theory* 21.1 (1975), pp. 15–23.
- [13] T. Kailath. “An RKHS approach to detection and estimation problems—I: Deterministic signals in Gaussian noise”. In: *IEEE Transactions on Information Theory* 17.5 (1971), pp. 530–549.
- [14] Kan Li and Jose C. Principe. *No-Trick (Treat) Kernel Adaptive Filtering using Deterministic Features*. 2019. arXiv: 1912.04530.
- [15] Weifeng Liu. “Extended Kernel Recursive Least Squares Algorithm”. In: *IEEE Transactions on Signal Processing* 57.10 (2009), pp. 3801–3814.
- [16] Weifeng Liu. “The Kernel Least-Mean-Square Algorithm”. In: *IEEE Transactions on Signal Processing* 56 (Mar. 2008), pp. 543–554.
- [17] Weifeng Liu, Jose C. Principe, and Simon Haykin. *Kernel Adaptive Filtering: A Comprehensive Introduction*. 1st. Wiley Publishing, 2010.
- [18] Yuqi Liu. “A Polarized Random Fourier Feature Kernel Least-Mean-Square Algorithm”. In: *IEEE Access* 7 (2019), pp. 50833–50838.

- [19] C H López-Caraballo. “Mackey-Glass noisy chaotic time series prediction by a swarm-optimized neural network”. In: *Journal of Physics: Conference Series* 720.1 (May 2016), p. 012002.
- [20] Edward Norton Lorenz. “Deterministic nonperiodic flow”. In: *Journal of the Atmospheric Sciences* 20 (1963), pp. 130–141.
- [21] Michael C. Mackey and Leon Glass. “Oscillation and Chaos in Physiological Control Systems”. In: *Science* 197.4300 (1977), pp. 287–289.
- [22] Charles A. Micchelli, Yuesheng Xu, and Haizhang Zhang. “Universal Kernels”. In: *Journal of Machine Learning Research* 7.95 (2006), pp. 2651–2667.
- [23] Mattes Mollenhauer et al. “Kernel Autocovariance Operators of Stationary Processes: Estimation and Convergence”. In: *Journal of Machine Learning Research* 23.327 (2022), pp. 1–34. URL: <http://jmlr.org/papers/v23/20-442.html>.
- [24] Krikamol Muandet et al. “Kernel Mean Embedding of Distributions: A Review and Beyond”. In: *Foundations and Trends® in Machine Learning* 10.1–2 (2017), pp. 1–141. ISSN: 1935-8245.
- [25] Emanuel Parzen. “An Approach to Time Series Analysis”. In: *The Annals of Mathematical Statistics* 32.4 (1961), pp. 951–989.
- [26] Emanuel Parzen. “Statistical Inference on time series by Hilbert Space Methods”. In: *Technical Report* (1959).
- [27] Zhengda Qin. “Augmented Space Linear Models”. In: *IEEE Transactions on Signal Processing* 68 (2020), pp. 2724–2738.
- [28] Ali Rahimi and Benjamin Recht. “Random Features for Large-Scale Kernel Machines”. In: *Advances in Neural Information Processing Systems*. Vol. 20. Curran Associates, Inc., 2007.
- [29] Carl Edward Rasmussen and Christopher K. I. Williams. *Gaussian processes for machine learning*. Adaptive computation and machine learning. MIT Press, 2006.
- [30] Friedrich Riesz. “Sur les systèmes orthogonaux de fonctions”. In: *Comptes rendus de l’Académie des sciences* 144 (1907), pp. 615–619.
- [31] Bernhard Schölkopf and Alexander J. Smola. *Learning with kernels : support vector machines, regularization, optimization, and beyond*. Adaptive computation and machine learning. MIT Press, 2002.

- [32] Shahrokh Shahi, Flavio H. Fenton, and Elizabeth M. Cherry. “Prediction of chaotic time series using recurrent neural networks and reservoir computing techniques: A comparative study”. In: *Machine Learning with Applications* 8 (2022), p. 100300. ISSN: 2666-8270.
- [33] A. N. Shiryayev. “Selected Works of A. N. Kolmogorov: Volume II Probability Theory and Mathematical Statistics”. In: Springer Netherlands, 1992. Chap. Stationary Sequences in Hilbert Space, pp. 228–271.
- [34] Bharath K. Sriperumbudur, Kenji Fukumizu, and Gert R.G. Lanckriet. “Universality, Characteristic Kernels and RKHS Embedding of Measures”. In: *Journal of Machine Learning Research* 12.70 (2011), pp. 2389–2410.
- [35] P. Stoica and Y. Selen. “Model-order selection: a review of information criterion rules”. In: *IEEE Signal Processing Magazine* 21.4 (2004), pp. 36–47.
- [36] Steven Van Vaerenbergh and Ignacio Santamaría. “A comparative study of kernel adaptive filtering algorithms”. In: *2013 IEEE Digital Signal Processing and Signal Processing Education Meeting (DSP/SPE)*. 2013, pp. 181–186.
- [37] Grace Wahba. *Spline Models for Observational Data*. Society for Industrial and Applied Mathematics, 1990.
- [38] Norbert Wiener. *Extrapolation, Interpolation, and Smoothing of Stationary Time Series*. New York: Wiley, 1949.
- [39] Norbert Wiener. *Ueber eine Klasse singulärer Integralgleichungen*. Sitzungsber. Akad. Wiss. Berlin, 1931.
- [40] Christopher Williams and Carl Rasmussen. “Gaussian Processes for Regression”. In: *Advances in Neural Information Processing Systems*. Ed. by D. Touretzky, M.C. Mozer, and M. Hasselmo. Vol. 8. MIT Press, 1995.
- [41] Changjiang Yang, Ramani Duraiswami, and Larry S Davis. “Efficient Kernel Machines Using the Improved Fast Gauss Transform”. In: *Advances in Neural Information Processing Systems*. Ed. by L. Saul, Y. Weiss, and L. Bottou. Vol. 17. MIT Press, 2004.